Research article

Journal of MASS SPECTROMETRY

Received: 8 June 2012 Revised: 13 July 2012 Accepted: 22 July 2012 Published online in Wiley Online Library

(wileyonlinelibrary.com) DOI 10.1002/jms.3068

Analysis of chloroquine and metabolites directly from whole-body animal tissue sections by liquid extraction surface analysis (LESA) and tandem mass spectrometry

Whitney B. Parson,[a] Stormy L. Koeniger,[b] Robert W. Johnson,[b] Jamie Erickson,[c] Yu Tian,[c] Christopher Stedman,[c] Annette Schwartz,[c] Edit Tarcsa,[c] Roderic Cole[c] and Gary J. Van Berkel[a]*

The rapid and direct analysis of the amount and spatial distribution of exogenous chloroquine (CHQ) and CHQ metabolites from tissue sections by liquid extraction surface sampling analysis coupled with tandem mass spectrometry (LESA-MS/MS) was demonstrated. LESA-MS/MS results compared well with previously published CHQ quantification data collected by organ excision, extraction and fluorescent detection. The ability to directly sample and analyze spatially resolved exogenous molecules from tissue sections with minimal sample preparation and analytical method development has the potential to facilitate the assessment of target tissue penetration of pharmaceutical compounds, to establish pharmacokinetic/pharmacodynamic relationships, and to complement established pharmacokinetic methods used in the drug discovery process during tissue distribution assessment. Copyright © 2012 John Wiley & Sons, Ltd.

Keywords: tissue analysis; imaging; mass spectrometry; chloroquine; surface sampling; LESA

Introduction

During drug development, information on the absorption, distribution, metabolism and excretion of each chemical entity is obtained to support human pharmacokinetics (PK) predictions, efficacy and safety evaluations. These studies typically entail analysis of the amount and distribution of the pharmaceutical compound and its metabolites in tissues by direct chemical imaging techniques[1,2] or by liquid chromatography coupled to mass spectrometry (LC-MS).[3,4] The standard method for direct, quantitative chemical imaging of pharmaceutical compounds in tissue sections is quantitative whole-body autoradiography (QWBA).[1,2] This technique detects the radiation of a radioactive label incorporated into the pharmaceutical compound and allows for assessment of quantitative spatial distribution. However, it has the disadvantage of not differentiating the pharmaceutical compound from its potential metabolites that might also carry the label; therefore, it requires secondary evaluation of excreta or tissues to measure radioactivity in high performance liquid chromatography (radio-HPLC) eluates coupled to MS detection.

LC-MS of unlabeled compounds is also widely utilized during drug discovery and development to assess the PK of drug candidates.[5–8] The high molecular specificity and low detection limits of MS provides the ability to analyze compounds directly from a wide variety of complex biological samples. However, due to the complexity of biological sample matrices, separation techniques such as LC are used subsequent to extraction of the exogenous compounds from the tissues, but prior to MS analysis to resolve isobaric species and increase sensitivity and dynamic range. While this workflow provides robust quantitative data, there is a considerable amount of method optimization for each individual compound to determine extraction efficiencies and matrix effects; at the same time, it provides only limited spatial resolution.

The development of novel MS-based methods able to rapidly assess the relative amounts, spatial distribution and metabolism of unlabeled pharmaceutical compounds with minimal sample preparation and method optimization would enable drug discovery programs to have *in vivo* tissue PK information early in the decision making process. This could also facilitate evaluation of target tissue penetration and PK/pharmacodynamics (PD) model development by understanding drug (and metabolite) concentrations directly at the biophase.[9–12] When these methods are effectively integrated into established approaches

* *Correspondence to: Gary J. Van Berkel, Organic and Biological Mass Spectrometry Group, Chemical Sciences Division, Oak Ridge National Laboratory, Oak Ridge, TN. E-mail: vanberkelgj@ornl.gov*

a *Organic and Biological Mass Spectrometry Group, Chemical Sciences Division, Oak Ridge National Laboratory, Oak Ridge, TN*

b *GPRD, Advanced Technology, Abbott Laboratories, Abbott Park, IL*

c *Drug Metabolism and Pharmacokinetics, Abbott Laboratories, Worcester, MA*

Journal of MASS SPECTROMETRY

used in drug discovery, their high spatial resolution combined with high specificity can quickly address questions regarding penetration of compound and potential metabolites to various tissues of interest that established methods could not or could only determine in later stages of development once radiolabeled compound becomes available.

New approaches to obtain direct molecular analysis of drugs and metabolites in tissue are maturing and expanding.[2,13–15] The most prominent and widely developed imaging approach to date has been matrix assisted laser desorption/ionization (MALDI)-MS.[16–21] With the intense investment in MALDI-based imaging in both the academic and industrial sectors, both the value and limitations of this technology have quickly become apparent.[2,22] With MALDI-based imaging, there remains a need for tissue preparation prior to analysis including, but not always limited to, a chemical matrix application and, typically, a need to carry out the analysis in the vacuum chamber of the mass spectrometer. Additionally, variable tissue type matrix effects can impede the quantitative value of the analysis and therefore limit the analytical applicability of the approach.

To overcome these challenges associated with MALDI-based imaging, new approaches to mass spectrometric imaging have been evaluated using atmospheric pressure surface sampling and ionization combinations in concert with mass spectrometric detection.[23–25] For example, desorption electrospray ionization (DESI)-MS uses a gas/liquid droplet spray plume to sample material from a surface by a liquid extraction process with subsequent ionization of the species in the rebounding extract containing droplets by an ESI-like process.[26,27] Compared to MALDI-MS, DESI-MS imaging offers the possibility to limit the amount of post-sectioning-tissue preparation and removes the vacuum constraints on the size and types of samples analyzed.

MALDI, DESI and other mass-spectrometry based surface sampling/ionization techniques can also be used in a spatially resolved profiling mode (*versus* an imaging mode) when fine spatially resolved chemical information is not required. Blatherwick *et al.*[28] recently argued that time-efficient profile or region analysis may be more appropriate to answer key questions around drug localization in a fit-for-purpose manner than generating time-intensive molecular images. In support of this claim, they presented profile data from tissue section analysis that employed two different implementations of a direct liquid extraction surface sampling probe, one of which is commercially available.[23] The commercially available sampling probe utilizes a robotic autosampler coupled with nanoelectrospray ionization (nanoESI) to perform discrete spot sampling by using a pipette tip to both dispense and retrieve a solution droplet directly from a surface sampling area approximately 1.5 mm in diameter.[29] This approach, termed liquid extraction surface analysis (LESA), coupled with MS has now been utilized in a number of studies to determine the amount, spatial distribution, and metabolism of pharmaceutical compounds directly from tissue sections without the requirement for sample preparation.[28–32] The workflow of the LESA-MS/MS experiment has been previously described.[29] Briefly, a liquid microjunction is formed with surfaces by dispensing a small amount of extraction solvent (~1.5 μL) from a single-use pipette tip. Analytes on the surface are then extracted into the solvent which is drawn back into the pipette tip. The pipette tip is then coupled to a microfabricated nanoESI chip containing single-use nozzles and introduced into the MS. Single use pipette tips and spray nozzles provides for zero carryover sample to sample.

In the work described here, the direct analysis of pharmaceutical compounds from tissue sections by LESA-MS/MS is applied to rapidly determine the relative amounts, spatial distribution and metabolism of chloroquine (CHQ, Scheme 1) in an acute time-course study. CHQ, a drug well studied over the past 50 years, has been used in the prevention and treatment of malaria and for autoimmune disorders such as rheumatoid arthritis.[33] The major metabolites (Scheme 1) are hydroxychloroquine (OH-CHQ) and desethylchloroquine (DESE-CHQ). Recently, CHQ measurements in ocular tissues of rats were shown to be consistent when measured by MALDI-MS and autoradiography.[34] In this work, it is shown that LESA-MS/MS is able to detect CHQ and the expected metabolites directly from whole-body animal tissue sections. Previously published data of CHQ distribution in treated rats correlates well with LESA-MS/MS data as well the plasma concentrations determined in this study by traditional LC-MS methods. These results illustrate that LESA-MS/MS can provide rapid and accurate measurements of the relative amounts of CHQ and metabolites directly from tissue sections without the requirement for extensive sample preparation such as tissue homogenization and HPLC separations.

Experimental

Materials

Hexane, LC-MS grade methanol (MeOH), 0.1% formic acid (FA) in acetonitrile (ACN) and 0.1% FA in water were purchased from Fisher Scientific (Pittsburgh, PA, USA). Carboxymethyl cellulose (CMC), hydroxypropyl methylcellulose (HPMC), ACN, dexamethasone and TWEEN 80 were purchased from Sigma Aldrich (St. Louis, MO, USA). CHQ, CHQ-d4, OH-CHQ and DESE-CHQ were purchased from Toronto Research Chemicals (NorthYork, Ontario, Canada).

Animal dosing

Male Sprague–Dawley® (SD) rats were purchased from Charles River Laboratories, Inc. (Kingston, NY, USA) and housed and treated under protocols approved by the Institutional Animal Care and Use Committee and according to the Guide for the Care and Use of Laboratory Animals.[35] SD rats were administered CHQ (10 mg/kg; p.o. in 0.02% TWEEN 80 in 0.5% HPMC) and euthanized via carbon dioxide gas at 2, 6 and 24 h post-dose ($N = 1$/timepoint). For whole-body tissue analysis, whole rats were immediately frozen in a dry ice/hexane bath (−80 °C) for 15–20 min, removed and dried of hexane, and stored overnight at −80 °C until embedded for

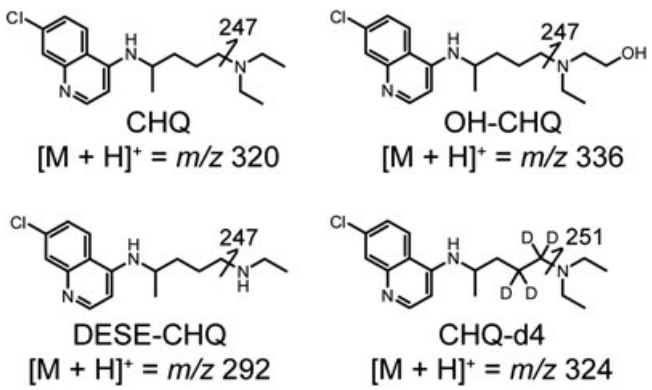

Scheme 1. Molecular structures, mass-to-charge values and the major product ion used for SRM are shown for CHQ, the isotope labeled compound, CHQ-d4, and the compound metabolites OH-CHQ and DESE-CHQ.

sectioning the next day. Whole blood (150 μL) was collected into heparin-prepared tubes (BD Bioscience, Bedford, MA, USA) from each animal at 0.25, 0.5, 1, 2, 4, 6, 12 and 24 h post-dose until the time of sacrifice. Plasma was immediately extracted via centrifugation of whole blood at 14 000 g at 4 °C for 5 min. A 100 μL aliquot of plasma was transferred into a clean tube and stored at −80 °C until further processing.

Sample preparation of plasma and whole-body tissue sections

Sample preparation procedures for plasma were automated using a TECAN robotic liquid handling system. CHQ was extracted from 20 μL of plasma via protein precipitation with 180 μL of ACN containing 200 nM of dexamethasone. Samples were centrifuged at 4000 rpm (4 °C) for 10 min, and then 50 μL of supernatant was collected and diluted with 50 μL of 35/65 (v/v) ACN/H_2O for MS analysis. A standard curve of eight concentrations was generated at final concentrations of 3 nM to 10 μM in control plasma. Standards in control plasma were processed identically to samples from treated animals. The extraction efficiency was 90%.

Whole body animals were prepared for sectioning by embedding into 2% CMC, sectioned with a Leica CM3600 cryomacrotome (Leica Microsystems, Bannockburn, IL, USA) at −20 °C onto acetate cryotape (3 M, St.Paul, MN, USA), dehydrated and stored at −80 °C until MS analysis. Discrete ~1.5 mm diameter areas were analyzed by LESA-MS/MS from the organs of interest for each compound from sagittal whole-body tissue sections (40-μm-thick).

Automated liquid extraction-based surface sampling and mass spectrometry

Tissue sections were analyzed on a TriVersa NanoMate (Advion Biosciences, Inc. Ithaca, NY, USA) with the LESA ($LESA_{Clarity}$) software package coupled to a 4000 QTRAP mass spectrometer (AB Sciex, Concord, Ontario, Canada). The extraction solvent used in all cases was 80/19.9/0.1 (v/v/v) ACN:H_2O:FA. A 2 μL volume of solvent was drawn up into the pipette tip. Volumes dispensed onto and aspirated back from the surface were both 1.5 μL. Extraction time was 1 s. A nanoESI voltage of 1.52 kV, and the gas pressure of 0.6 psi was applied in all experiments. The nanoESI flow rate was estimated to be ~330 nL/min. Mass spectral data were acquired and averaged over 1 min via selected reaction monitoring (SRM). Dwell times were 50 ms for all SRM transitions.

Plasma concentrations by traditional LC-MS analysis

LC-MS analysis of plasma samples was performed on a 4000 QTRAP mass spectrometer coupled to an Agilent 1100 Series LC (Foster City, CA, USA). Plasma extracts were analyzed for CHQ concentrations by injecting 10 μL onto a Waters Xtera MS18 column (2.1 X 30 mm, Milford, MA, USA). The analytes were eluted at 850 μL/min with a 0–95% gradient of ACN with 0.2% FA over 0.5 min followed by a 1.4 min wash at 95% ACN with 0.2% FA and a total run time of 1.9 min. Positive ion mode SRM was used for the analysis of CHQ (*m/z* 320.0 → 247.0) and the internal standard dexamethasone (*m/z* 393.2 → 147.1). Precursor and product ions were transmitted at unit resolution, and product ions were produced with a collision energy of 25 eV for CHQ and 15 eV for dexamethasone.

Results and discussion

To evaluate the feasibility of measuring exogenous compounds and metabolite concentrations directly from tissue sections, a drug with well-known pharmacokinetics and metabolite profile i.e. CHQ), was selected.[36–38] CHQ has a very large volume of distribution and has been associated with renal toxicity.[39,40] Tissue pharmacokinetics of CHQ were evaluated following oral dosing (10 mg/kg) in male rats. The optical image of a whole-body tissue section on acetate tape (2 h post-dose) is shown in Fig. 1a, where the various organs analyzed in this work (liver, lung, spleen and kidney) are outlined and labeled. The data presented in Figs. 1b and 1c illustrate the ability to definitively detect CHQ sampled directly from the tissue using LESA and tandem mass spectrometry. Figure 1b shows the averaged enhanced product ion (EPI) spectrum of the precursor ion at *m/z* 320 obtained from a 100 nM CHQ standard ($(M+H)^+ = m/z$ 320) by direct nanoESI infusion. Two dominant and expected product ions were observed at *m/z* 247 and 142 (see Scheme 1).[41] Figure 1c shows the EPI spectrum from *m/z* 320 obtained when analyzing by LESA-MS/MS a spot in the liver of the treated whole-body animal tissue section shown in Fig. 1a. The product spectra in Fig. 1b and 1c are nearly identical indicating that CHQ was effectively extracted from the tissue and subsequently ionized and detected by LESA-MS/MS. In comparing the product ion signal for *m/z* 247 in Figs. 1b and 1c, it is possible to estimate the amount of CHQ in the dosed-animal tissue section. The product ion signal was 2.5 times higher from the tissue than from the standard solution indicating that the concentration of CHQ in the extract exceeded 100 nM. From an analysis of tissue matrix signal suppression (see in discussion on internal standard recovery), signal suppression presumably contributed at least a tenfold diminution in the signal of the extract compared to the standard solution. Assuming a linear signal *versus* concentration response, the concentration of CHQ can be estimated in the LESA extract to be as high as 2.5 μM. Extracting CHQ from a discrete location into a small volume (~1.5 μL) concentrates the analyte and therefore improves the limit of detection. It is important to note that in methods using whole organ tissue homogenization, regions of high concentration will be diluted by regions of low concentration thereby not only decreasing the overall concentration of analyte in the organ, but also masking potentially high accumulation of compound or metabolites in localized regions of the organ.

Extracts of different tissues are known to have variable matrix components that reflect the tissue composition and may impact the degree of ionization in ESI differently. To understand the matrix effects in LESA across multiple tissue types, the signal level of the deuterated internal standard, CHQ-d4, was used to evaluate ionization suppression effects in organs of interest (e.g. kidney, lung liver, and spleen). CHQ-d4 was spiked into the extraction solvent at 100 ηM. The signal resulting from direct infusion of extraction solvent was compared before and after a 1 s extraction from each organ type on a control whole-body tissue section. The results, presented in Fig. 2, show that the CHQ-d4 signal in the presence of matrix was on average 8% of the intensity of the signal observed if the same solution was sprayed without performing the extraction. Though the signal was suppressed by approximately an order of magnitude with the matrix present, the CHQ-d4 signal suppression observed was not significantly different among the various organs. CHQ signal from the lung tissue extraction had the largest relative standard deviation (RSD) in the percent recovered signal, which is believed to be due to the heterogeneous nature of lung tissue. Assuming the extraction efficiencies of the metabolites from the

Journal of MASS SPECTROMETRY

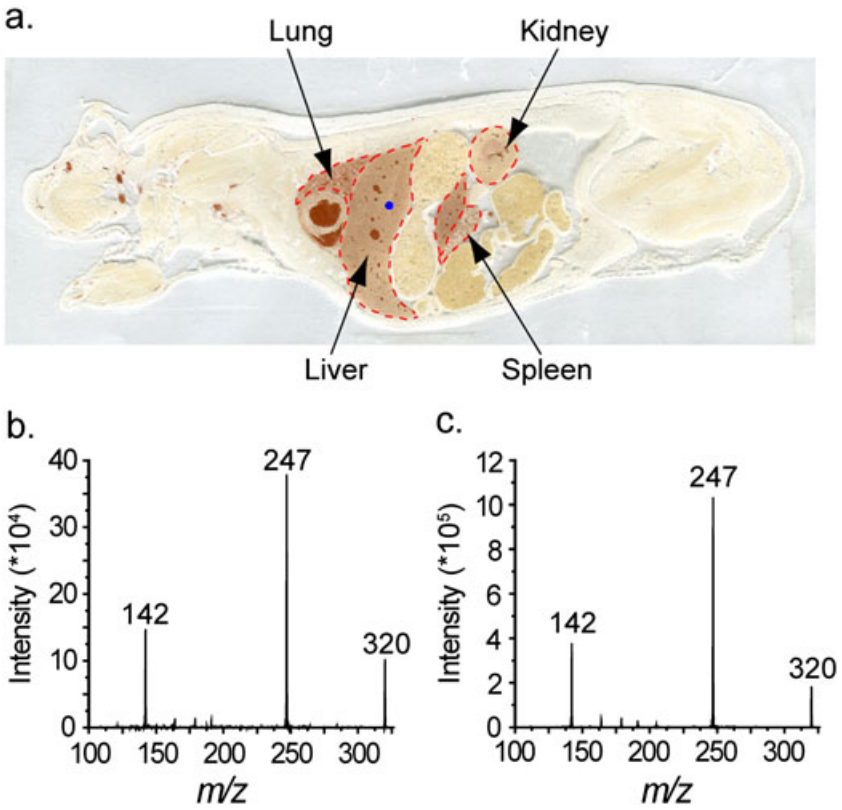

Figure 1. Direct analysis of CHQ from animal-dosed tissue sections by LESA-MS/MS. (a) Optical image of a CHQ dosed rat (10 mg/kg CHQ p.o.; 2 h post-dose) whole-body tissue section (~40 μm) on acetate tape with analyzed organs (liver, lung, spleen and kidney) outlined and labeled. Averaged EPI spectrum (1 min acquisition) of the precursor ion at *m/z* 320 from (b) a 100 nM CHQ standard ($(M+H)^+ = m/z$ 320) by direct nanoESI infusion and from (c) a sampled spot in the liver of the tissue section shown in (a) by LESA-MS/MS. The blue dot in the optical image indicates the sampled spot location (~1 mm in diameter).

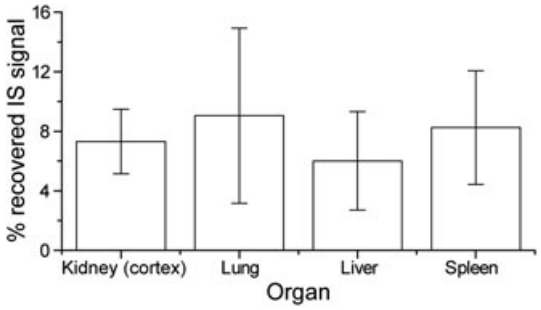

Figure 2. LESA-MS/MS evaluation of signal suppression from matrix effects in different tissue types. LESA-MS/MS was performed by spiking an internal standard (CHQ-d4, 100 ηM) into the extraction solvent (80/19.9/0.1 (v/v/v) ACN:H_2O:FA) and measuring the signal level of CHQ-d4 from the analysis of multiple tissue types (kidney cortex, lung, liver and spleen) compared to direct infusion nanoESI-MS for each analyte standard. LESA-MS/MS analysis was performed on three areas per tissue type and on three serial tissue sections per time-point ($N = 9$/tissue type). Results are reported as the percent recovered signal from each organ.

different tissue types are similar for CHQ or CHQ-d4, the relative signal levels observed should correlate well with the absolute amounts of material present in the areas examined.

Another question related to the LESA analysis was the origin of the observed variability of CHQ and metabolite signal from the same organ within a tissue. This signal variation has two main components one being inherent to the reproducibility of the extraction and nanoESI process and another related to real biological spatial distribution of the targeted compounds within the tissue. Of particular interest was the observation of significant differences in CHQ and metabolite signal reproducibility among the different tissue types that were being sampled. Tissues that are generally homogenous, such as liver, were typically observed to have lower standard deviations from different locations within the tissue than heterogeneous tissue types, such as the lung. To determine if these variations were due to real spatial distribution differences, the CHQ signal was compared between areas sampled within an organ (lung and liver) or the same area from three serial tissue sections. If the standard deviation was due to organ heterogeneity, then the standard deviation should be smaller from the same area on three serial tissue sections than the standard deviation for combined measurements from all three locations from the same organ within a given tissue section. The optical image for the three serial sections is shown in Fig. 3a. Tissue sections 1 and 3 were both over-laid with section 2 (middle), and the same areas were chosen for LESA-MS/MS analysis of CHQ from the liver and lung tissues in each section. For the liver, the combined average CHQ signal for all areas and sections compared well with the averaged signal levels for each of the individual areas and the average RSD was ~17%. This is consistent with the RSDs (8.5%, 30.7% and 11.8%) measured for the three separate areas on the same serial sections (Fig. 3b); therefore the spatial variation in the amount of CHQ at the different locations in the liver on a 1.5 mm diameter area is in the range of the variability in the extraction process (~8–30%) and nanoESI (~5–10%) process.

The situation for the lung was different due to the spongy and highly heterogenous anatomy of this organ. Overall, the standard deviations for all areas of the lung region except area 2 had

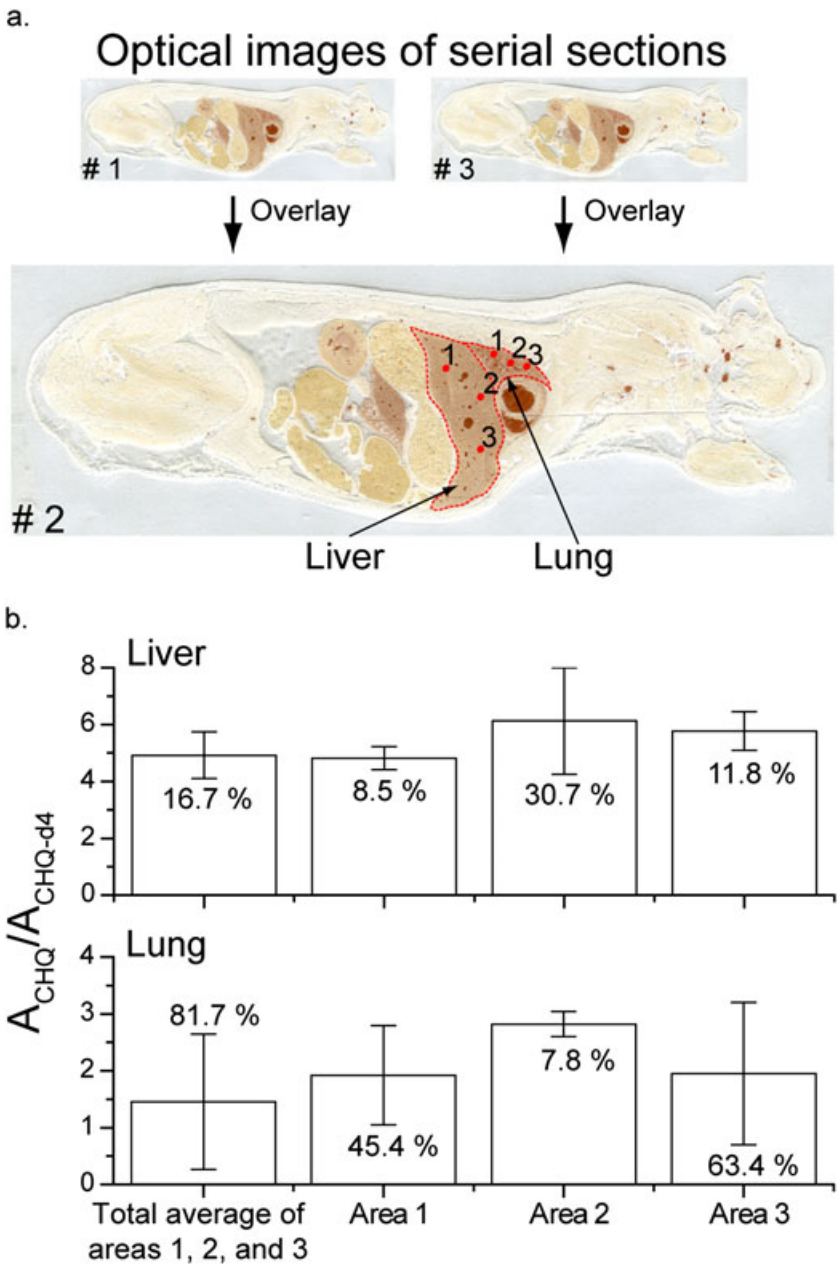

Figure 3. Determination of technical and spatial variation of CHQ in different tissue types. The same area from three serial sections of a 10 mg/kg (p.o.; 2 h post-dose) CHQ dosed rat were analyzed by LESA-MS/MS. (a) The optical images for tissue sections 1 and 3 were over-laid with 2 (middle section), and from each section, the same three areas were selected for LESA-MS/MS analysis from the liver and lung. (b) CHQ (*m/z* 320 → 247) signals obtained via integration of the SRM transitions were normalized to the internal standard, CHQ-d4, integrated for the entire acquisition and averaged for serial sections of the liver (top) and the lung (bottom) for each area analyzed. The average and RSD for each area on three serial sections is reported independently as well as the average and RSD for all measurements from each area and serial section (Total average of areas 1, 2 and 3).

greater RSDs than any of the liver regions. This higher variability may be attributed to differences in the formation of the liquid junction at the lung tissue surface which, unlike the liver, has a variable ratio of tissue and non-tissue (e.g. tape) regions created from the airways in the lung. The combined average RSD from the lung was ~82% for all the areas and serial sections compared to 45%, 8% and 63% obtained for each area 1, 2 and 3, respectively. This large variation in the combined average signal level was indicative of spatial variation in the amounts of CHQ present.

The ability of LESA-MS/MS to analyze surfaces in a spatially resolved manner, albeit at relatively low resolution, was further demonstrated using kidney samples. CHQ is known to be eliminated to a large extent by renal tubular secretion. LESA-MS/MS analysis was performed along a sequential series of points (2 mm center-to-center spacing) across the renal cortex and medulla of the kidney section (Fig. 4a). The actual area sampled was evident by the color change in the tissue where the extraction solvent contacted the tissue surface (Fig. 4b). Each spot analyzed was approximately 1.5–2 mm in diameter. In this case, the relatively large sampling spot size and spacing was still sufficient to distinguish the difference in signal intensity, and therefore CHQ content, between these two regions in the kidney (Fig. 4c). In general, the intra-renal distribution of pharmaceutical compounds is variable depending on the compound class and physical health

Journal of MASS SPECTROMETRY

of the kidney.[42] In this study, CHQ was found in greater amounts in the medulla region compared to the cortex. The differential distribution of drug and metabolites in these two distinct regions of the kidney has also been observed with other drugs using MALDI-MS imaging.[18,43,44]

LESA-MS/MS was employed in a 24 h time-course study to measure the change in tissue distribution of CHQ and its metabolites, DESE-CHQ and OH-CHQ, following administration of a single dose of CHQ (10 mg/kg; p.o.). CHQ, DESE-CHQ and OH-CHQ were analyzed by SRM in the liver, lung, spleen and the cortex of the kidney at 2, 6 and 24 h post-dose. CHQ, DESE-CHQ and OH-CHQ were detected in all tissues analyzed (Fig. 5); however, the medulla was excluded from this analysis due to the inability to consistently measure it at all timepoints and replicates. In all examined tissues, the amount of CHQ maximized at 6 h post-dose then decreased with various rates. The amount of DESE-CHQ measured increased with time up to 24 h in all analyzed tissue types. The results for OH-CHQ were more varied, due, in part, to the low concentration of this metabolite in the analyzed tissues. OH-CHQ levels increased in all tissue types up to 6 h and then remained constant or slightly increased in the spleen and kidney (cortex) between 6 and 24 h. Without taking into account possible differential extraction and ESI response factors for CHQ and the different metabolites, these results correlated with previous tissue distribution results in that the metabolite signals from tissue were approximately 10% of those recorded for CHQ.[37] To ensure proper dosing and compliment LESA-MS/MS data in this time-course study, plasma was collected from rats at multiple time points until their time of sacrifice and analyzed for CHQ content (Fig. 6). All animals ($N = 3$/group) showed a two- to three- fold increase in CHQ concentrations in the plasma between 0.25 and 2 h post administration of CHQ with C_{max} in plasma reaching ~6 h post-dose, similar to what was observed for the tissues by LESA-MS/MS.

To evaluate LESA-MS/MS analysis against previously published data, a comparison was performed for the 24 h time point (Fig. 7). CHQ tissue distribution studies by Varga[36] (20 mg/kg) and by McChesney, *et al.*[37] (40 mg/kg) each of which used organ excision, extraction and fluorescent detection for CHQ quantification correlated well with LESA-MS/MS measurements. The order of increasing tissue concentrations of CHQ (e.g. kidney $<$ liver $\leq$ lung $<$ spleen) was consistent with these two previous reports for measurements 24 h post administration of a single dose. To make this comparison, the relative amounts of CHQ in the kidney, lung and spleen were normalized to that of the liver. This result indicates that LESA-MS/

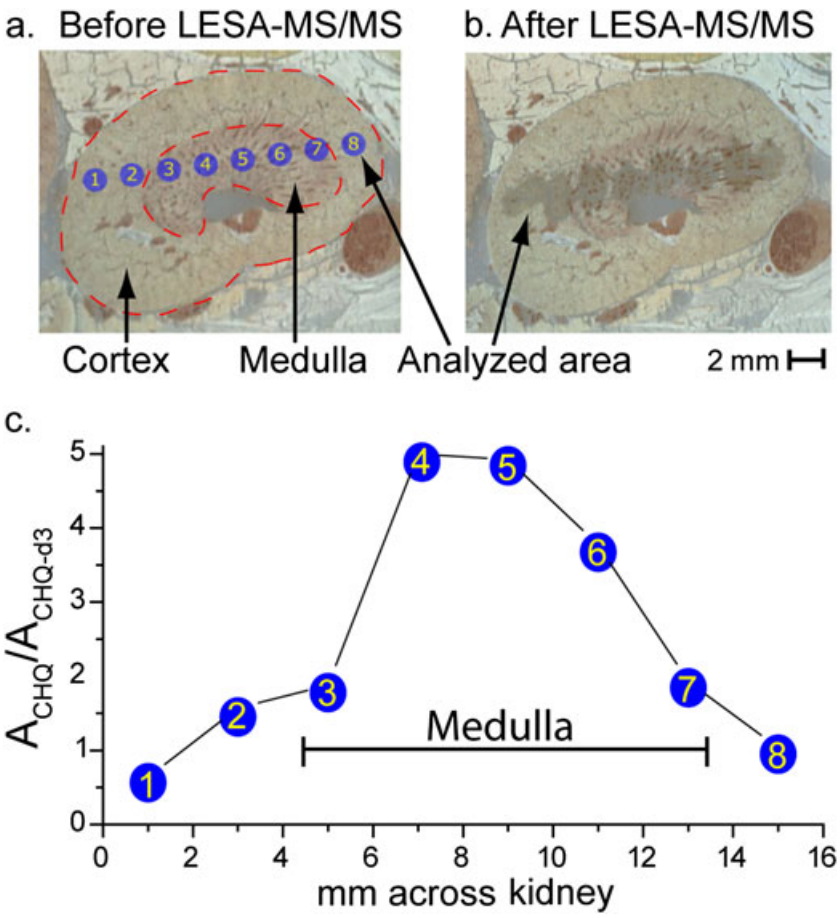

Figure 4. Spatial distribution of CHQ in the kidney from a CHQ-dosed animal (10 mg/kg; 2 h) tissue section. (a) Optical image of the kidney tissue section prior to LESA-MS/MS analysis. The numbered blue circles were created using $LESA_{Clarity}$ software (1 mm diameter with 2 mm center-to-center spacing) and indicate selected LESA-MS/MS analysis points. (b) Optical image of kidney section after LESA-MS/MS analysis illustrating the actual areas analyzed across the cortex and medulla (outlined by red dashes in (a) of the kidney). Each analysis spot was approximately 1.5–2 mm in diameter. (c) Integrated SRM signals of CHQ normalized to the internal standard, CHQ-d4, are plotted *versus* distance in mm across the kidney section. The numbered blue circles correlate with the numbered circles in (a) and indicate the intensity *versus* spatial location in the cortex (circles 1, 2 and 8) and the medulla (circles 3–7).

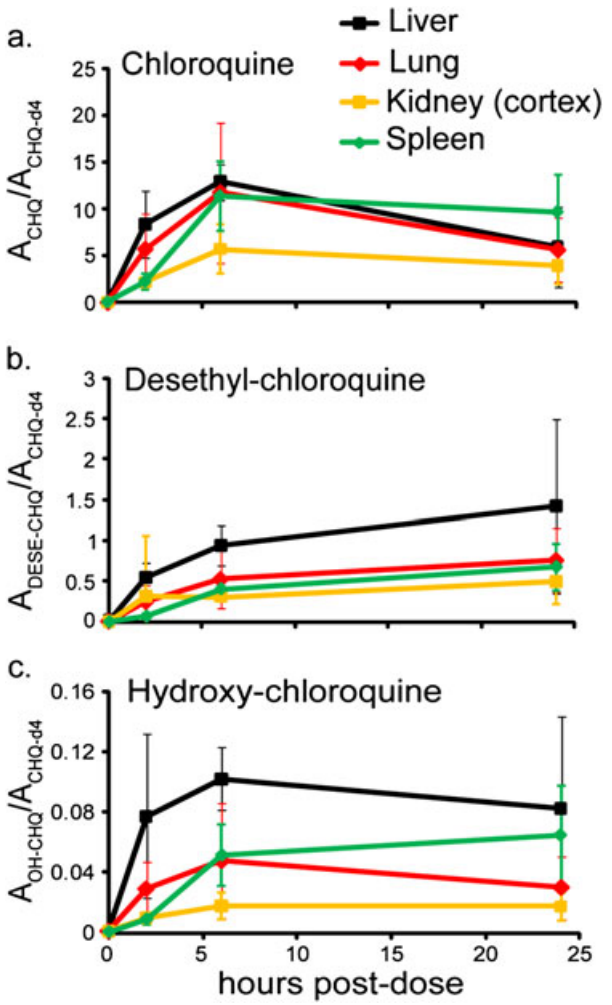

Figure 5. A 24 h time-course study of the relative amounts, spatial distribution and metabolism of CHQ directly from dosed-animal tissue sections. LESA-MS/MS analysis was performed from three areas per tissue type and from three serial tissue sections per time-point ($N = 9$ per tissue type at each time-point). For each area analyzed, the SRM signals were integrated for the length of the acquisition and normalized to the internal standard, CHQ-d4. The average normalized values of (a) CHQ, (b) DESE-CHQ and (c) OH-CHQ are reported as a function of hours post-dose in the liver (black), lung (red), kidney (yellow) and spleen (green).

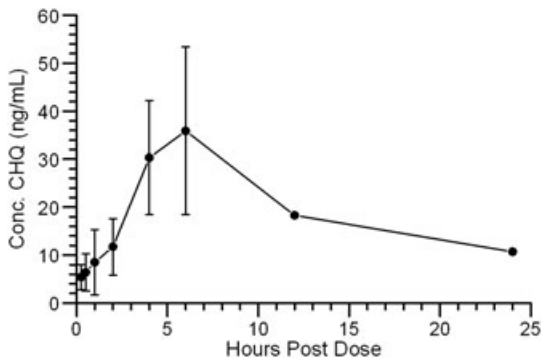

Figure 6. CHQ concentration measured in plasma collected from rats at multiple post-dose time points until their time of sacrifice ($N = 3$/group).

MS was able to rapidly provide accurate relative tissue distributions of exogenous pharmaceutical compounds similar to other analytical techniques commonly utilized for PK analysis.

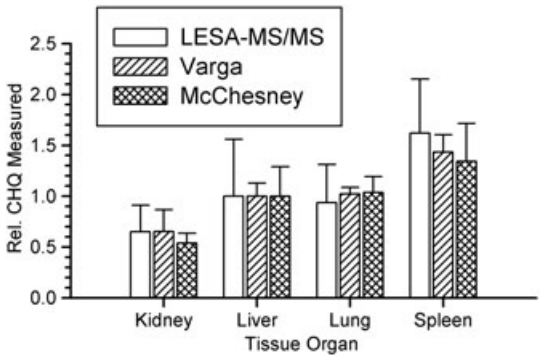

Figure 7. Comparison of the relative CHQ tissue distribution reported in the literature and determined by LESA-MS/MS in this work. To make this comparison, all data was normalized with respect to the levels of CHQ reported in the liver of the respective study. For LESA-MS/MS, rats were dosed with 10 mg/kg CHQ and sacrificed at 24 h post-dose. For each area analyzed, the SRM signals were integrated for the length of the acquisition and normalized to the internal standard, CHQ-d4. The average normalized values for each organ are shown. (open bars; LESA-MS/MS analysis; nine technical replicates). For the data obtained by Varga,[36] rats were dosed with 20 mg/kg CHQ and sacrificed at 24 h post-dose (striped bars; UV spectroscopy; eight biological replicates). For the data obtained by McChesney,[37] rats were dosed with 40 mg/kg CHQ and sacrificed at 24 h post-dose (cross-hatch bars; UV spectroscopy; four biological replicates).

Conclusions

The development and validation of MS-based methods able to rapidly provide data that can be used to determine the relative amounts, spatial distribution and metabolism of unlabeled or labeled pharmaceutical compounds will enable early evaluation of tissue PK in drug discovery and compliment established PK/PD methods in drug development. In laboratories with established processing capabilities (e.g. tissue sectioning) for QWBA, LESA-MS/MS can be quickly integrated as a 'plug-n-play' process to deliver complementary data or address questions unforeseen by radiolabeled methods. In bioanalytical laboratories with established LC-MS processes, resources for tissue sectioning will be the largest barrier to obtaining higher resolution tissue distribution data; however, this can be minimized by focusing on the organs of interest instead of the whole body. As an MS-based method, LESA-MS/MS analysis provides a wide dynamic range and does not require a matrix or additional processing of the tissue post sectioning. In this study, LESA-MS/MS directly measured the relative abundance of CHQ as well as the expected metabolites in multiple tissue types and observed no differential tissue matrix effects for CHQ across tissue types. Previously published data on CHQ tissue distributions for rats compared well with the LESA-MS/MS data.

One current limitation of this technology compared to other existing surface sampling approaches is in regard to the spatial resolution (currently ~1.5–2 mm in diameter). This is inherent in the use of a pipette tip and the solvent system used for extraction. The use of smaller size pipette tips is being explored, but it will inevitably be a balance between spatial resolution and the sensitivity required for the analysis. In the LESA-MS/MS approach, one can quickly change the pipette size or the solvent used for extraction and therefore the spatial resolution of the analysis. Additionally, while MS acquisition for each spot sampled on a tissue was performed over 1 min for this study, the acquisition time can be significantly extended (up to 30 mins) using low flow chips for the Triversa nanomate. Extended analysis times

would facilitate the search for unknown metabolites allowing time-consuming-dependent MS/MS, precursor ion or neutral loss scans to be performed on demand.[45] Currently, LESA-MS/MS as well as many other surface sampling approaches for mass spectrometry imaging are limited to qualitative or relative quantitation and the development of robust absolute quantitation methods are still in their infancy. However, similar issues (e.g. tissue thickness, density of tissue type, temperature, exposure, etc.) beset the integrity of QWBA before it was more widely accepted in the field of pharmacology.[1,2,46–48]

Acknowledgements

Work at Oak Ridge National laboratory (ORNL) was funded by a Work for Others Agreement with Abbott Laboratories, Chicago, IL and Worcester, MA.

References

[1] E. G. Solon, S. K. Balani, F. W. Lee. Whole-Body Autoradiography in Drug Discovery. *Curr. Drug Metab.* **2002**, *3*(5), 451–62.
[2] E. G. Solon, A. Schweitzer, M. Stoeckli, B. Prodeauz. Autoradiography, MALDI-MS, and SIMS-MS Imaging in Pharmaceutical Discovery and Development. *AAPS J.* **2010**, *12*, 11–26.
[3] M. Honing. The Role of LC-MS in Drug Discovery and Development, an Overview. In *The Encyclopedia of Mass Spectrometry*, Vol. *8*, M. L. Gross, R. M. Caprioli (Eds). Elsevier, Ltd.: Oxford, UK, **2006**, 393–401.
[4] M. Holčapek, L. Kolářová, M. Nobilis. High-Performance Liquid Chromatography Tandem Mass Spectrometry in the Identification and Determination of Phase I and Phase II Metabolites. *Anal. Bioanal. Chem.* **2008**, *391*, 59–78.
[5] R. Kostiainen, T. Kotiaho, T. Kuuranne, S. Auriola. Liquid chromatography/atmospheric pressure ionization-mass spectrometry in drug metabolism studies. *J. Mass Spectrom.* **2003**, *38*, 357–372.
[6] W. A. Korfmacher. Foundation review: Principles and applications of LC-MS in new drug discovery. *DDT* **2005**, *10*, 1357–1367.
[7] R. N. Xu, L. Fan, M. J. Rieser, T. A. El-Shourbagy. Recent advances in high-throughput quantitative bioanalysis by LC-MS/MS. *J. Pharm. Biomed. Anal.* **2007**, *44*, 342–355.
[8] C. Prakash, C. L. Shaffer, A. Nedderman. Analytical strategies for identifying drug metabolites. *Mass Spectrom. Rev.* **2007**, *26*, 340–369.
[9] C. E. C. A. Hop, M. J. Cole, R. E. Davidson, D. B. Duignan, J. Federico, J. S. Janiszewski, K. Jenkins, S. Krueger, R. Lebowitz, T. E. Liston, W. Mitchell, M. Snyder, S. J. Steyn, J. R. Soglia, C. Taylor, M. D. Troutman, J. Umland, M. West, K. M. Whalen, V. Zelesky, S. X. Zhao. High throughput ADME screening: practical considerations, impact on the portfolio and enabler of in silico ADME models. *Curr. Drug Metab.* **2009**, *9*, 847–853.
[10] H. Gao, L. Yao, H. W. Mathieu, Y. Zhang, T. S. Maurer, M. D. Troutman, D. O. Scott, R. B. Ruggeri, J. Lin. In silico modeling of nonspecific binding to human liver microsomes. *Drug Metab. Dispos.* **2008**, *36*, 2130–2135.
[11] T. T. Wager, R. Y. Chandrasekaran, X. Hou, M. D. Troutman, P. R. Verhoest, A. Villalobos, Y. Will. Defining Desirable Central Nervous System Drug Space through the Alignment of Molecular Properties, in Vitro ADME, and Safety Attributes. *ACS Chem Neurosci* **2010**, *1*, 420–434.
[12] M. P. Gleeson, A. Hersey, S. Hannongbua. In-silico ADME models: a general assessment of their utility in drug discovery applications. *Curr. Top. Med. Chem.* (Sharjah, United Arab Emirates) **2011**, *11*, 358–381
[13] J. Pól, M. Strohalm, V. Havlíček, M. Volný. Molecular Mass Spectrometry Imaging in Biomedical and Life Science Research. *Histochem. Cell Biol.* **2010**, *134*, 423–443.
[14] R. J. A. Goodwin, A. R. Pitt. Mass Spectrometry Imaging of Pharmacological Compounds in Tissue Sections. *Bioanalysis* **2010**, *2*, 279–293.
[15] Y. Sugiura, M. Setou. Imaging Mass Spectrometry for Visualization of Drug and Endogenous Metabolite Distribution: Toward In Situ Pharmacometabolmes. *J. Neuroimmune Pharmacol.* **2010**, *5*, 31–43.
[16] S. R. Shanta, Y. Kim, Y. H. Kim, K. P. Kim. Application of MALDI Tissue Imaging of Drugs and Metabolites: A New Frontier for Molecular Histology. *Biomo. Ther.* **2011**, *19*, 149–154.
[17] B. Prideaux, V. Dartois, D. Staab, D. M. Weiner, A. Goh, L. E. Via, C. E., III Barry, M. Stoekli. High-Sensitivity MALDI-MRM-MS Imaging of Moxifloxacin Distribution in Tuberculosis-Infected Rabbit Lungs and Granulmatous Lesions. *Anal. Chem.* **2011**, *83*, 212–2118.
[18] D. S. Cornett, S. L. Frappier, R. M. Caprioli. MALDI-FTICR Imaging Mass Spectrometry of Drugs and Metabolites in Tissue. *Anal. Chem.* **2008**, *80*, 5648–5653.
[19] M. L. Reyzer, R. M. Caprioli. MALDI-MS-Based Imaging of Small Molecules and Proteins in Tissues. *Curr. Opin. Chem. Biol.* **2007**, *11*, 29–35.
[20] S. Khatib-Shahidi, M. Andersson, J. L. Herman, T. A. Gillespie, R. M. Caprioli. Direct Molecular Analysis of Whole-Body Animal Tissue Sections by Imaging MALDI Mass Spectrometry. *Anal. Chem.* **2006**, *78*, 6448–6456.
[21] M. L. Reyzer, Y. Hsieh, K. Ng, W. A. Korfmacher, R. M. Caprioli. Direct Analysis of Drug Candidates in Tissue by Matrix-Assisted Laser Desorption/Ionization Mass Spectrometry. *J. Mass Spectrom.* **2003**, *38*, 1081–1092.
[22] A. Svatos. Mass spectrometric imaging of small molecules. *Trends Biotechnol.*, **2010**, *28*, 425–434.
[23] G. J. Van Berkel, S. P. Pasilis, O. Ovchinnikova. Established and Emerging Atmospheric Pressure Surface Sampling/Ionization Techniques for Mass Spectrometry. *J. Mass Spectrom.* **2008**, *43*, 1161–1180.
[24] G. A. Harris, A. S. Galhena, F. M. Fernandez. Ambient Sampling/Ionization Mass Spectrometry: Applications and Current Trends. *Anal. Chem.* **2011**, *83*, 4508–4538.
[25] M.-Z. Huang, C.-H. Yuan, S.-C. Cheng, Y.-T. Cho, J. Shiea. Ambient Ionization Mass Spectrometry. *Annu. Rev. Anal. Chem.* **2010**, *3*, 43–65.
[26] V. Kertesz, G. J. Van Berkel, M. Vavrek, K. A. Koeplinger, B. B. Schneider, T. R. Covey. Comparison of Drug Distribution Images from Whole Body Thin Tissue Sections Obtained using Desorption Electrospray Ionization Tandem Mass Spectrometry and Autoradiography. *Anal. Chem.* **2008**, *80*, 5168–5177.
[27] J. M. Wiseman, D. R. Ifa, Y. Zhu; C. B. Kissinger, N. E. Manike, P. T. Kissinger, R. G. Cooks. Desorption Electrospray Ionization Mass Spectrometry: Imaging Drugs and Metabolites in Tissues. *PNAS* **2008**, *105*, 18120–18125.
[28] E. Q. Blatherwick, G. J. Van Berkel, K. Pickup, M. K. Johansson, M.-E. Beaudoin, R. O. Cole, J. M. Day, S. Iverson, I. D. Wilson, J. H. Scrivens, D. J. Weston. Utility of Spatially-Resolved Atmospheric Pressure Surface Sampling and Ionization Techniques as Alternatives to Mass Spectrometry Imaging (MSI) in Drug Metabolism. *Xenobiotica* **2011**, *41*, 720–734.
[29] V. Kertesz. G. J. Van Berkel. Fully Automated Liquid Extraction-Based Surface Sampling and Ionization using a Chip-Based Robotic Nanoelectrospray Platform. *J. Mass Spectrom.* **2010**, *45*(3), 252–60.
[30] P. Marshall, V. Toteu-Djomte, P. Bareille, H. Perry, G. Brown, M. Baumert, K. Biggadike. Correlation of Skin Blanching and Percutaneous Absorption for Glucocorticoid Receptor Agonists by Matrix-Assisted Laser Desorption Ionization Mass Spectrometry Imaging and Liquid Extraction Surface Analysis with Nanoelectrospray Ionization Mass Spectrometry. *Anal. Chem.* **2010**, *82*, 7787–7794.
[31] D. Eikel, M. Vavrek, S. Smith, C. Bason, S. Yeh, W. A. Korfmacher, J. D. Henion. Liquid Extraction Surface Analysis Mass Spectrometry (LESA-MS) as a Novel Profiling Tool for Drug Distribution and Metabolism Analysis: The Terfenadine Example. *Rapid Commun. Mass Spectrom.* **2011**, *25*, 3587–3596.
[32] S. Schadt, S. Kallbach, R. Almeida, J. Sandel. Investigation of Figopitant and its Metabolites in Rat Tissue by Combining Whole Body Autoradiography with Liquid Extraction Surface Analysis Mass Spectrometry. *Drug Metab. Dispos.* [Epub **2011** Dec 19]. doi:10.1124/dmd.111.043562
[33] M. Grundmann, P. Vrublovský, V. Demková, I. Mikulíková, E. Pěgřmová. Tissue Distribution and Urinay Excretion of Chloroquine in Rats. *Arzneim.-Forsch.* **1972**, *22*, 82–88.
[34] Y. Yamada, K. Hidefumi, H. Shion, M. Oshikata, Y. Haramaki. Distribution of Chloroquine in Ocular Tissue of Pigmented Rat using Matrix-Assisted Laser Desorption/Ionization Imaging Quadrupole Time-of-Flight Tandem Mass Spectrometry. *Rapid Commun. Mass Spectrom.* **2011**, *25*, 1600–1608.
[35] *Guide for the Care and Use of Laboratory Animals*, (8th Edn). The National Academies Press: Washington, DC, **2010**.
[36] F. Varga. Tissue Distribution of Chloroquine in the Rat. *Acta Phys. Acad. Sci. Hung. Tomas* **1968**, *34* (4): 319–325.

[37] E. W. McChesney, W. F. Banks, D. J. Sillivan. Metabolism of Chloroquine and Hydroxychloroquine in Albino and Pigmented Rats. *Tox. Appl. Pharm.* **1965**, *7*, 627–636.
[38] E. W. McChesney, W. F., Jr. Banks, J. P. McAuliff. Laboratory Studies of the 4-Aminoquinoline Antimalarials: II. Plasma Levels of Chloroquine and Hydroxychloroquine in Man after Various Oral Dosage Regimes. *Antibiot. Chemother.* **1962**, *12*, 583–594.
[39] L. L. Gustafsson, O. Walker, G. Alvan, B. $eermann, F. Estevez, L. Gleisner, B. Lindstrom, F. Sjoqvist. Disposition of Chloroquine in Man After Single Intravenous and Oral Doses. *Br. J. clin. Pharmac.* **1983**, *15*, 471–479.
[40] J.-L. Clemessy, S. W. Borron, F. J. Baud, C. Favier, P. E. Hantson, E. Vicaut. Hypokalaemia Related to Acute Chloroquine Ingestion. *Lancet* **1995**, *346*, 877–880.
[41] P. Singhal, A. Gaur, V. Behl, A. Gautam, B. Varshney, J. Paliwal, V. Batra. Sensitive and Rapid Liquid Chromatography/Tandem Mass Spectrometry Assay for the Quantification of Chloroquine in Dog Plasma. *J. Chromtogr. B* **2007**, *852*, 293–299.
[42] A. Whelton, W. G. Walker. Intrarenal Antibiotic Distribution in Health and Disease. *Kidney Int.*, **1974**, *6* 131–137.
[43] P. J. Trim, C. M. Henson, J. L. Avery, A. McEwen, M. F. Snel, E. Claude, P. S. Marshall, A. West, A. P. Princivalle, M. R. Clench. Matrix-Assisted Laser Desorption/Ionization-Ion Mobility Separation-Mass Spectrometry Imaging of Vinblastine in Whole Body Tissue Sections. *Anal. Chem.* **2008**, *80*, 8628–8634
[44] A. Römpp, S. Guenther, Z. Takats, B. Spengler. Mass Spectrometry Imaging with High Resolution in Mass and Space (HR2 MSI) for Reliable Investigation of Drug Compound Distributions on the Cellular Level. *Anal. Bioanal. Chem.* **2011**, *401*, 65–73.
[45] M. J. Walworth, M. S. ElNaggar, J. J. Stankovich, C. Witkowski; J. L. Norris, G. J. Van Berkel. Direct Sampling and Analysis from Solid-Phase Extraction Cards using an Automated Liquid Extraction Surface Analysis Nanoelectrospray Mass Spectrometry System. *Rapid Commun. Mass Spectrom.* **2011**, *25*(17): 2389–96.
[46] R. D. Irons, E. A. Gross. Standardization and Calibration of Whole-Body Autoradiography for Routine Semiquantitative Analysis of the Distribution of ^{14}C-Labeled Compounds in Animal Tissues. *Tox. Applied Pharmacology* **1981**, *59*, 250–256.
[47] S. A. M. Cross, A. D. Groves, T. Hesselbo. A Quantitative Method for Measuring Radioactivity in Tissues Sectioned for Whole-Body Autoradiography. *Int. J. Applied Rad. Isotopes* **1974**, *25*, 381–382.
[48] J. Maasa, R. Binderb, W. Steinkec. Quantitative Whole-Body Autoradiography: Recommendations for the Standardization of the Method. *Regul. Toxicol. Pharmacol.* **2000**, *31*, S15–S21.